

Circumstellar emission from dust envelopes around carbon stars showing the silicon carbide feature

A. Blanco, A. Borghesi, S. Fonti, and V. Orfino

Dipartimento di Fisica, Università di Lecce, Via per Arnesano C. P. 193, I-73100 Lecce, Italy

Received 28 January 1997 / Accepted 13 August 1997

Abstract. Spectroscopic and photometric data relative to a sample of 55 carbon stars showing the 11.3 μm feature have been fitted in the wavelength range between 0.4 and 100 μm by means of a radiative transfer model using the laboratory extinction spectra of amorphous carbon and silicon carbide (SiC) grains. The transfer code allows to determine in a self-consistent way the grain equilibrium temperature of the various species at different distances from the central star and gives all the relevant circumstellar parameters which can be very important for the evolutionary study of carbon stars.

In order to get meaningful information on the nature and physical properties of the dust grains responsible for the 11.3 μm feature and the underlying continuum, the fitting procedure of the spectra has been applied individually to every single source. For this reason it has been possible to take into account any variation in position and shape of the band from source to source.

Our analysis show that all the sources, in addition to the amorphous carbon grains accounting for the continuum emission, need always the presence of α -SiC particles while some of them require also β -SiC. Moreover, the presence of one or both types of SiC particles seems not correlated neither with the total optical thickness nor with any other physical and geometrical parameters of the circumstellar envelope.

The best-fit parameters found in this work have been used to calculate the mass-loss rate from the central stars. The clear correlation, that we find between the strength of the SiC feature and the total mass loss-rate, confirms the results already found by other authors for the same kind of sources and derived from the observed CO emission lines.

Key words: stars: carbon – stars: circumstellar matter – infrared: stars

1. Introduction

It is well known that a large amount of dust is produced in the envelopes of late-type stars (Jura 1985) and that a very important contribution comes from C-rich giant stars (Knapp & Morris 1985). The atmospheres of the latter type of sources are

generally thought to be the place where carbon and silicon carbide (SiC) grains can easily condense (Tielens 1990). The exact nature of the two solid components, however, is not yet well established and the debate on the allotropic form of carbon grains (amorphous or crystalline) as well as of the SiC component (α -SiC or β -SiC; Borghesi et al. 1985) is still alive. Recently a new classification scheme of the IRAS LRS carbon stars proposed by Goebel et al. (1995) identifies three distinct dust species: SiC, α :C-H, a type of hydrogenated carbon film (Dischler et al. 1983a,b) and MgS. It is clear therefore that a study of the infrared spectra of carbon stars may improve our knowledge on the formation processes and physical properties of the ejected dust particles and on the mass-loss outflow in the circumstellar shells (Skinner & Whitmore 1988; Groenewegen & de Jong 1991; Groenewegen 1995). Both processes are clearly related to the life history of carbon stars thought to be a direct evidence for evolution along the asymptotic giant branch (Chan & Kwok 1988, 1990; Willems 1988a).

The problem of the type of SiC grains formed in the outflows of carbon stars is of considerable interest also for the likely connections with solar system studies. Meteoritic specimens show the presence of a SiC component outside the confines of the carbon-rich circumstellar environments (Tang & Anders 1988; Zinner et al. 1989; Amari et al. 1992). Surprisingly all the SiC grains found in meteorites are β -SiC (Hoppe et al. 1994) while the majority of those present in the circumstellar envelopes seems to be α -SiC (Blanco et al. 1994; Groenewegen 1995; Speck et al. 1996).

In a previous paper (Blanco et al. 1994, hereinafter Paper I), we have fitted the infrared spectra of eight IRAS sources chosen among the brightest carbon stars and exhibiting a prominent circumstellar emission feature around 11.3 μm . We obtained good fits, between 8 and 20 μm , using the optical properties of a mixture of amorphous carbon (AC) and SiC submicronic grains, produced and characterized in our laboratory (Orfino et al. 1991). The extinction laboratory data were used as inputs for a simple theoretical model which simulated the dust envelope by means of a homogeneous and isothermal shell with a spherical geometry. We were able to determine the values of the best-fit parameters concerning the carbon stars and their cir-

cumstellar shells, but the main result was the clear possibility to discriminate between the sources containing only α -SiC and those containing both α -SiC and β -SiC. We also attempted an evolutionary interpretation of such diversity. The main problem was that the isothermal model prevented us from fitting the whole IRAS spectra up to 100 μm . Moreover, the number of sources was too small to allow any meaningful statistical analysis.

In this paper we extend the analysis to a larger number of carbon stars in a wider spectral range (0.4-100 μm). The aim is to clarify the open problems on the nature of the circumstellar dust and to provide a set of circumstellar parameters which can be very important for the evolutionary study of carbon stars. Moreover we use an improved radiative transfer model which allows to calculate the temperature profile across the shell for each component of the grain mixture.

It is important to note that the fitting procedure of the spectra is applied individually to every source. Indeed, as already stressed in Paper I, this is one of the leading condition in order to get meaningful information on the nature and physical properties of the dust grains responsible for the 11.3 μm feature and the underlying continuum. Moreover, the best-fit parameters can be used to evaluate the mass-loss rate from the central stars so that the results can be compared with those derived by means of completely independent methods as the observations of CO emission lines.

In Sect. 2 we define the carbon star sample and report the leading criteria used for the choice of the infrared sources. In Sect. 3 is presented a description of the radiative transfer code used for the model calculations, whose results are reported in Sect. 4. Finally discussion and conclusions are reported in Sect. 5.

2. The carbon star sample

For our detailed study we have considered the observational data concerning 55 carbon stars (see Table 1). The basic criteria for the choice have been two: a) the availability of photometric and spectroscopic observational data in the widest possible wavelength range and b) the clear presence of well defined SiC bands.

Following Willems (1988a, 1988b) we started with the 90 carbon stars for which both the visible-infrared photometry (Noguchi et al. 1981; Hoffleit & Jaschek 1982; Gezary et al. 1987; Stephenson 1989) and the IRAS Low Resolution Spectra (LRS; IRAS Science Team 1986) were available. The number of sources to be analysed has been then reduced to 55 taking into account the requested presence of the SiC band, since some of the IRAS-LRS spectra either do not exhibit the 11.3 μm emission feature or show a band too weak and noisy for the purposes of the present analysis. In fact, it is worthwhile to point out that for our study we had to take into account the individual spectra with their detailed shape and position of the SiC band while Willems (1988a, 1988b) groups, in his analysis, these sources in two classes according to the optical thickness of the circumstellar envelope. He rightfully assumes an average peak position of 11.3 μm for the optically thick class and 11.6 μm for the optically thin one.

However, the peak position varies of more than 0.5 μm within each class and therefore the exact determination of the nature of the dust grains requires the sources to be fitted individually. To do this care has to be taken to deal with both laboratory and observational data.

3. Best-fit model calculation

As reported in the introduction, the simplified model used in Paper I allowed us to fit quite well the spectra of some IRAS sources in the wavelength range 8 - 20 μm . However, when we tried to extend the fit up to 100 μm , we found that an isothermal shell was not able to account for the emission in the whole spectrum. To overcome this problem we have adopted an improved model based on a radiative transfer code developed by Egan et al. (1988) using the so-called "quasi diffusion method" (Leung 1975, 1976a, 1976b). In this model the total flux emitted by a spherical circumstellar dust envelope is evaluated, taking also into account the effects due to first-order scattering, by means of the energy balance equation between absorption and emission at each point inside the envelope. This allows to calculate in a self-consistent way the equilibrium temperature of the grains of the various species at different distances from the central star. The model, although originally developed for modelling of dust in molecular clouds and star formation regions, has already been tested and successfully applied to the case of the circumstellar envelopes of late-type stars (Le Bertre 1988; Chan & Kwok 1990; Egan & Leung 1991).

The input parameters of this model are: the star temperature T_* ; the optical thickness τ of the envelope at 5500 Å; the ratios R_I/R_* and R_E/R_I , where R_* is the stellar radius while R_I and R_E are the inner and outer radius of the envelope, respectively. The model allows also to change the exponent γ of the grain number density law, $n_g \propto r^{-\gamma}$, but we worked with a fixed value of $\gamma = 2$ which, as shown by Kömpe et al. (1995), has been found to be appropriate for the envelopes around carbon stars. As far as the inner radius of the envelope is concerned, it is worthwhile to note that some authors prefer to fix it by using the condition that at $r = R_I$ the grain temperature is equal to the condensation temperature T_c of the considered chemical species. We preferred, instead, to keep the parameter R_I/R_* free and to take into consideration that grain nucleation and growth around cool stars can occur only when the gas reaches distances from the star much larger than those where $T = T_c$. This conclusion has been suggested by interferometric observations of Mira variables (Beckwith 1985) and can be probably explained by the presence of strong instabilities in the stellar outflow (Tielens & Allamandola 1987). Taking into account this situation in our case the temperature at the inner boundary of the envelope is not fixed but it is calculated by the model (see Fig. 1 for a specific example). In any case we discarded those best fits obtained with a temperature at the inner radius which was larger than 1500 K. Moreover, the fits we obtained in this way are generally better than those obtained when R_I/R_* is fixed by the condensation temperature. Similar conclusions have been obtained also by Orofino et al. (1990) in the case

Table 1. The carbon star sample

IRAS name	NAME	SPT	IRC	RAFGL	CS	3 μm	8.6 μm	14 μm
00172+4425	VX And	C4,5J	+40006	50	11	c	c	c
00248+3518	AQ And	C5,4	+40010	68	16	a	–	b
01080+5327	HV Cas	C4,3E	+50030	167	56	b	–	a
01105+6241			+60041	177	59	c	a	–
01133+2530	Z Psc	C7,2	+30025	188	63	a	–	b
01531+5900	X Cas	C5,4E	+60069	270S	87	c	c	c
03229+4721			+50096	489	142	b	–	–
03374+6229	U Cam	C5,4	+60124	505	154	b	a	–
03377+5120	V466 Per	C5,5	+50100	507	155	a	–	–
03415+4437	AC Per	C6,3	+40067		157	a	–	c
04459+6804	ST Cam	C5,4	+70055	633	240	a	–	–
04483+2826	TT Tau	C7,4	+30098	639	254	a	–	a
04573-1452	R Lep	C7,4E	-10080	667	276	c	–	–
05028+0106	W Ori	C5,4	+00066	683	284	b	b	b
05056+3856	TX Aur	C5,4	+40115		288	a	–	–
05185+3227	UV Aur	C8,1JE	+30100	735	318	c	a	–
05238+3406	S Aur		+30114	748	336	c	a	–
05426+2040	Y Tau	C6,3	+20121	5168	393	a	–	–
05576+3940	AZ Aur	C7,1E	+40151	853	433	c	–	–
06149+0832	GK Ori	C5,4	+10113	910	480	b	c	c
06192+0722	BN Mon	C4,3E	+10118	920	498	b	–	b
06331+3829	UU Aur	C6,4	+40158	966	537	a	–	–
06529+0626	CL Mon	C6,3E	+10144	1038	615	c	–	–
06556+0614	RV Mon	C4,4	+10146	1044	632	a	–	–
07045-0728	RY Mon	C5,5	-10149	1070	670	b	b	b
07057-1150	W CMa	C6,3	-10152	1075	676	a	–	–
07270-1921			-20131	1131	776	b	–	–
07487-0229			+00162	1199	918	c	–	–
08174+0255	RY Hya	C6,4E	+00172	1243	1123	b	b	b
08525+1725	X Cnc	C5,4	+20206	1298	1338	a	a	a
08538+2002	T Cnc	C5,5	+20207	1301	1344	b	c	b
10416+6740	VY UMa	C6,3	+70100	1433	1736	a	–	a
12226+0102	SS Vir	C5,3E	+00217	1549	1999	c	b	b
12427+4542	Y CVn	C5,5J	+50219	1576	2030	a	–	–
12447+0425	RU Vir	C8,1E	+00224	1579	2032	c	a	–
12544+6615	RY Dra	C4,5J	+70116	1588	2047	a	a	–
16239-1218	V Oph	C7,3E	-10339	1859	2334	a	b	a
16374-3217	SU Sco	C5,5	-30268	1878	2353	b	b	b
17556+5813	T Dra	C6,2E	+60255	2040	2512	b	–	–
18306+3657	T Lyr	C6,5J	+40321	2187	2608	c	c	c
18410+3654	HK Lyr	C7,4	+40325	2240	2651	a	–	–
18562+1417	UV Aql	C5,3	+10389	2292	2684	a	–	a
19008+0726			+10401	2310	2694	a	a	–
19017-0545	V Aql	C5,4	-10486	2314	2695	a	a	a
19147+2149	CG Vul		+20393	2358	2717	a	–	a
19184+3746	U Lyr	C4,5E	+40354	5367S	2724	a	a	–
19272+4556	AW Cyg	C4,5	+50295	2396	2739	a	a	a
19416+3422			+30385	2443	2783	b	a	–
19555+4407	AX Cyg	C4,5	+40368	2480	2833	a	a	–
20028+2030	X Sge		+20452	2504	2853	a	–	c
20082+2911			+30416	5473S	2871	b	a	b
20472+3302		C6,4	+30456	5547S	2935	a	–	a
21035+5136			+50357	2704	2976	a	b	–
21320+3850	V1426 Cyg		+40485	2781	3041	a	–	–
21399+3516	V460 Cyg	C6,3	+40489	2793	3060	a	–	a

¹Notes: NAME and SPT are the name and the spectral type from Yamashita (1972, 1975). IRC and RAFGL are respectively the identifications of the sources in the two-micron Infrared Sky Survey (Neugebauer & Leighton 1969) and in the Revised Air Force Geophysical Laboratory (Price & Murdock 1983) catalogs. CS is the number in the General Catalogue of Cool Carbon Stars (Stephenson 1989). The last three columns indicate the presence and intensity (a - weak, b - intermediate, c - strong) of the very common bands at 3, 8.6 and 14 μm

of the very well known object IRC+10216 and by Groenewegen (1995) for a sample of 21 carbon stars by using different radiative transfer models.

Other important model parameters are the extinction and scattering cross sections and the scattering asymmetry factor of the dust grains in the spectral range $0.1 - 5000 \mu\text{m}$, and the relative amount of each component of the mixture. We have used a three components mixture of AC, α -SiC and β -SiC submicronic grains, whose mean size are $0.008 \mu\text{m}$, $0.04 \mu\text{m}$ and $0.02 \mu\text{m}$ respectively. The extinction cross sections of these grains have been obtained starting from the experimental values of Q_{ext}/a (where Q_{ext} is the extinction efficiency of the grains and a their average radius). These have been determined for AC in the spectral range $0.1 - 300 \mu\text{m}$ (Bussoletti et al. 1987) and between 2.5 and $300 \mu\text{m}$ for α -SiC and β -SiC (Borghesi et al. 1985; Borghesi et al. 1986). For all the materials the extrapolation up to $5000 \mu\text{m}$ has been performed by using the same spectral index determined in the 100 - $300 \mu\text{m}$ region. For both types of SiC particles the extrapolation to $0.1 \mu\text{m}$ has been obtained by using Mie theory and the optical constants of α -SiC given by Pégourié (1988). Moreover, since the experimental extinction spectra have been obtained with the grains embedded in a pellet of potassium bromide (KBr), we had to take into account matrix effects in order to obtain the values of Q_{ext}/a in vacuum (Orofino et al. 1991). This has been done by extrapolating the experimental values of Q_{ext}/a in KBr by means of Mie theory and using the optical constants of AC (Rouleau & Martin 1991) and SiC (Pégourié 1988) grains.

The scattering cross sections and the asymmetry factor of the SiC grains have been calculated again with Mie theory starting from the optical constants of this material (Pégourié 1988). We have assumed that the scattering of AC particles is negligible since the size of these particles is much smaller than the wavelength in the whole spectral range of interest. Moreover the ultraviolet component of the stellar radiation is small due to the very low temperatures of the stars of our sample.

4. Results

In Fig.1 are shown the radial trends of the temperature calculated for the different grain components taken inside a typical optically thin ($\tau = 0.1$) envelope with $R_I/R_E = 10^{-3}$ around a star with a temperature $T_* = 2600 \text{ K}$. We have found that for AC particles these numerically determined temperature profiles are well fitted (differences less than 3%) by the law $T_d(r) \propto r^{-f}$, where $f = 2/(4 + \beta)$ and $\beta = 0.95$ is the average spectral index of the grain opacity in the IR, that is in the region where the dust emission is strongest. On the contrary, for the SiC grains the temperature does not follow a power law due to the presence in the IR of the strong absorption band around $11.3 \mu\text{m}$. The same conclusions hold for non optically thin envelopes.

In Table 2 we report the values of the best-fit parameters used in modelling each source. In some cases we preferred to choose those best-fit curves that, besides an overall good fit, could give values of best-fit parameters close to those available in the literature and obtained with other methods. In particular

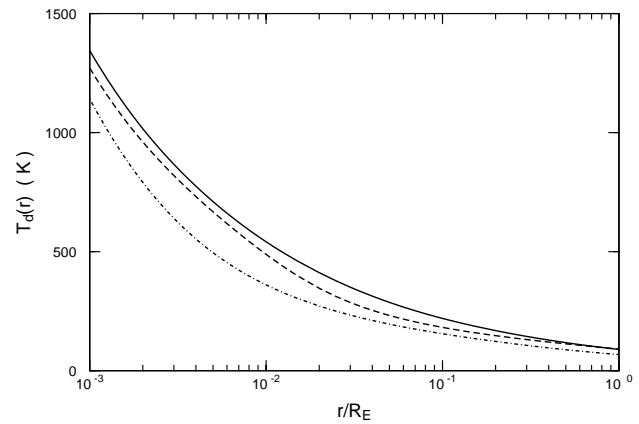


Fig. 1. Radial trends of the temperature calculated for the different grain components (*solid line*: AC; *dashed line*: α -SiC; *dot-dashed line*: β -SiC) taken inside a typical optically thin envelope ($\tau = 0.1$) around a star with $T_* = 2600 \text{ K}$

the optical thicknesses τ have been checked against the existence of an optical counterpart. It is worthwhile to note that the envelopes around the four J-type stars in the sample have low optical thicknesses, in agreement with the spectral classification of Keenan & Morgan (1941).

As it can be seen from Table 2 and in agreement with Paper I, all the sources have been best fitted by a mixture composed of AC, responsible for the continuum emission, and α -SiC grains. 22 sources (40% of the total) need also the presence of β -SiC particles in significant amounts. The best-fit abundances of the various components, expressed in terms of mass, are reported only in steps of 5% for sake of homogeneity, even if some of the sources, with clear and noiseless spectra, could have been fitted with more precise percentages.

Figs. 2 and 3 show two examples of the typical best fits of the emission spectra of two sources of the sample (namely IRAS 04573-1452 and IRAS 06331+3829), in the wavelength ranges $0.1 - 100 \mu\text{m}$ (a) and $8-20 \mu\text{m}$ (b). Since the IRAS data at 25 , 60 and $100 \mu\text{m}$ were obtained with broad bandpass filters (Gezary et al. 1987), we have calculated for all sources the color correction factors necessary to obtain flux values at the effective wavelength of the filters. The color temperatures, T_{ij} , were determined between adjacent IRAS bands i and j and the correction factors were derived by interpolation using correction factors listed in table VI.C.6 of the IRAS Catalog and Atlas Explanatory Supplement (Beichman et al. 1988). For bands (25 and $60 \mu\text{m}$) with two adjacent bands two correction factors have been calculated and averaged.

The fits are generally quite good with the major discrepancies appearing in the blue ($0.43 \mu\text{m}$) and visible ($0.55 \mu\text{m}$) part of the spectra. In this wavelength region for most of the objects the maximum discrepancy, between theoretical curves and observational spectra, lies within a factor 4.5, with only 6 exceptions where it can reach a maximum value of 17. The poor quality of the fits in this region, which seems to be in common also with other similar works (Chan & Kwok 1990; Groenewegen

Table 2. Best-fit model parameters of our IRAS source sample and computed mass-loss rates (in solar masses per year)

IRAS name	τ	$T_*(\text{K})$	R_I/R_*	R_E/R_I	AC(%)	$\alpha\text{SiC}(\%)$	$\beta\text{SiC}(\%)$	\dot{M}
00172+4425	0.1	2500	5.0	10^4	85	15	–	$1.2 \cdot 10^{-7}$
00248+3518	0.1	2800	3.0	10^3	75	25	–	$1.3 \cdot 10^{-7}$
01080+5327	0.4	1600	3.0	10^2	75	15	10	$7.8 \cdot 10^{-7}$
01105+6241	1.5	1600	3.0	10^2	75	15	10	$2.9 \cdot 10^{-6}$
01133+2530	0.1	2900	3.2	10^3	75	25	–	$1.5 \cdot 10^{-7}$
01531+5900	0.1	2550	4.0	10^4	75	20	5	$1.2 \cdot 10^{-7}$
03229+4721	0.8	1500	5.0	10^3	75	15	10	$3.5 \cdot 10^{-6}$
03374+6229	0.3	2400	3.0	10^4	75	20	5	$2.2 \cdot 10^{-7}$
03377+5120	0.2	2450	4.0	10^4	90	10	–	$1.6 \cdot 10^{-7}$
03415+4437	0.1	2400	4.0	10^4	75	25	–	$9.9 \cdot 10^{-8}$
04459+6804	0.1	2700	3.4	10^3	80	20	–	$1.2 \cdot 10^{-7}$
04483+2826	0.1	2750	3.0	10^3	90	10	–	$8.8 \cdot 10^{-8}$
04573-1452	0.8	1800	3.0	10^3	75	15	10	$9.2 \cdot 10^{-7}$
05028+0106	0.1	2500	4.0	10^4	75	25	–	$1.1 \cdot 10^{-7}$
05056+3856	0.2	2700	5.0	10^4	90	10	–	$2.8 \cdot 10^{-7}$
05185+3227	0.7	2400	5.0	10^3	90	10	–	$6.4 \cdot 10^{-7}$
05238+3406	0.8	1750	2.6	10^3	75	25	–	$9.0 \cdot 10^{-7}$
05426+2040	0.3	2700	3.5	10^4	80	20	–	$3.6 \cdot 10^{-7}$
05576+3940	0.6	1850	3.0	10^3	75	15	10	$6.1 \cdot 10^{-7}$
06149+0832	0.1	2400	4.0	10^4	75	25	–	$9.9 \cdot 10^{-8}$
06192+0722	0.3	2350	3.2	10^4	75	20	5	$2.2 \cdot 10^{-7}$
06331+3829	0.2	2700	3.5	10^4	85	15	–	$2.1 \cdot 10^{-7}$
06529+0626	0.5	2000	4.2	10^3	75	15	10	$5.0 \cdot 10^{-7}$
06556+0614	0.1	3000	4.0	10^3	75	25	–	$2.2 \cdot 10^{-7}$
07045-0728	0.2	2600	3.2	10^3	75	15	10	$2.1 \cdot 10^{-7}$
07057-1150	0.1	3200	5.0	10^3	75	25	–	$3.4 \cdot 10^{-7}$
07270-1921	1.0	1700	3.0	10^3	80	20	–	$1.3 \cdot 10^{-6}$
07487-0229	1.2	1600	2.0	10^2	90	10	–	$1.1 \cdot 10^{-6}$
08174+0255	0.5	2500	2.6	10^3	75	15	10	$3.7 \cdot 10^{-7}$
08525+1725	0.1	2600	2.7	10^3	75	15	10	$8.9 \cdot 10^{-8}$
08538+2002	0.2	2500	3.0	10^4	75	15	10	$1.7 \cdot 10^{-7}$
10416+6740	0.2	2950	4.8	10^3	75	25	–	$4.9 \cdot 10^{-7}$
12226+0102	0.3	2600	3.0	10^4	75	15	10	$3.0 \cdot 10^{-7}$
12427+4542	0.2	2550	4.3	10^4	85	15	–	$2.2 \cdot 10^{-7}$
12447+0425	0.9	1900	5.0	10^2	75	15	10	$1.3 \cdot 10^{-6}$
12544+6615	0.1	2800	3.0	10^3	90	10	–	$9.4 \cdot 10^{-8}$
16239-1218	0.1	2800	3.0	10^3	75	25	–	$1.3 \cdot 10^{-7}$
16374-3217	0.1	2500	5.0	10^4	85	15	–	$1.2 \cdot 10^{-7}$
17556+5813	0.8	1700	5.0	10^2	75	15	10	$2.0 \cdot 10^{-6}$
18306+3657	0.1	2400	4.0	10^4	85	15	–	$8.1 \cdot 10^{-8}$
18410+3654	0.1	2500	3.4	10^3	75	15	10	$9.8 \cdot 10^{-8}$
18562+1417	0.1	2600	2.7	10^3	75	15	10	$8.9 \cdot 10^{-8}$
19008+0726	1.8	1300	3.5	10^2	90	10	–	$7.7 \cdot 10^{-6}$
19017-0545	0.1	2500	3.5	10^3	80	20	–	$9.1 \cdot 10^{-8}$
19147+2149	0.2	2400	3.0	10^3	80	20	–	$1.3 \cdot 10^{-7}$
19184+3746	0.3	2500	3.4	10^4	75	15	10	$2.9 \cdot 10^{-7}$
19272+4556	0.1	2600	3.0	10^3	75	15	10	$9.9 \cdot 10^{-8}$
19416+3422	1.2	1600	2.0	10^2	90	10	–	$1.1 \cdot 10^{-6}$
19555+4407	0.1	2500	3.5	10^4	80	20	–	$9.1 \cdot 10^{-8}$
20028+2030	0.1	2750	3.0	10^3	75	25	–	$1.2 \cdot 10^{-7}$
20082+2911	1.2	1500	2.5	10^2	75	10	15	$2.6 \cdot 10^{-6}$
20472+3302	0.2	2500	4.6	10^4	75	25	–	$2.6 \cdot 10^{-7}$
21035+5136	1.5	1300	3.5	10^3	75	25	–	$8.7 \cdot 10^{-6}$
21320+3850	0.6	1550	3.0	10^4	75	25	–	$1.3 \cdot 10^{-6}$
21399+3516	0.1	3000	4.0	10^3	75	15	10	$2.2 \cdot 10^{-7}$

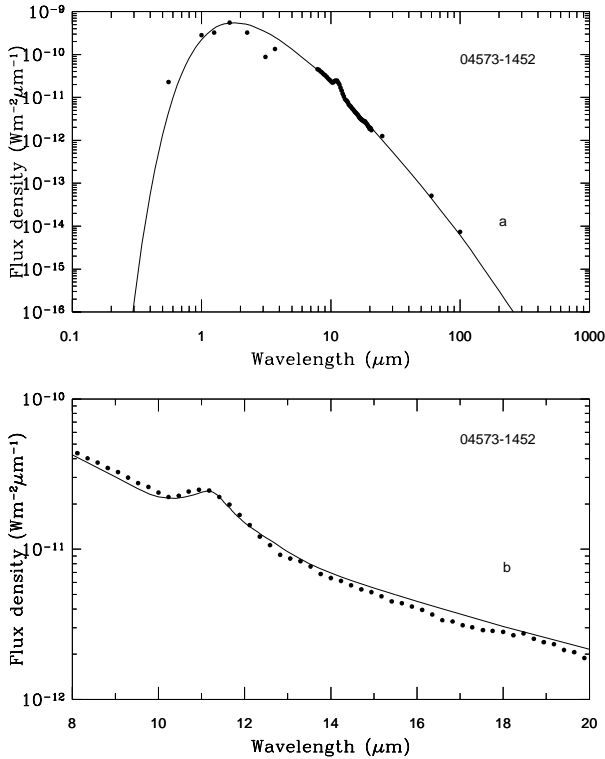


Fig. 2. Typical best-fit curves (*solid line*) of the observed photometric and spectroscopic data (*dots*) relative to the source IRAS 04573-1452.

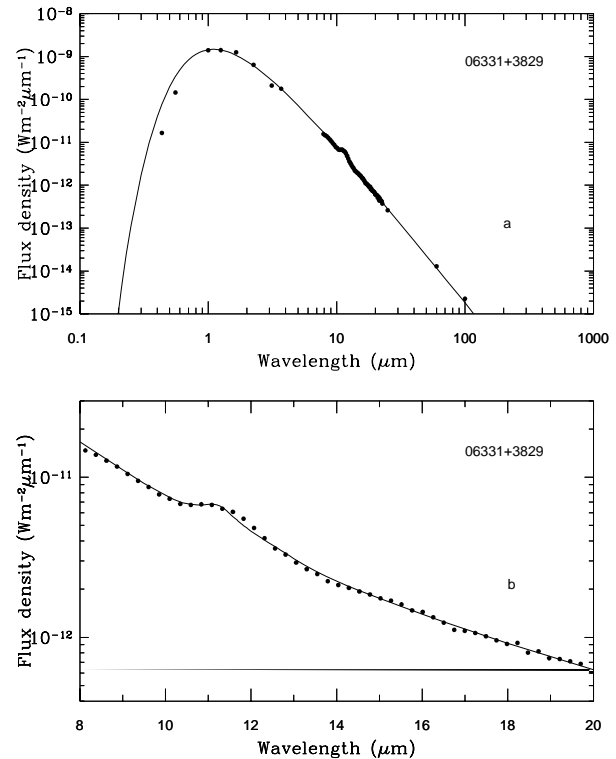


Fig. 3. Same as Fig. 2 but for the source IRAS 06331+3829.

1995) is due to a compromise in obtaining better results in the infrared part of the spectrum. We have also to consider the fact that the high variability of this kind of sources influences mainly the blu and visible fluxes. We recall for instance, that in Mira variables the flux at maximum can be up to 250 times the flux at minimum.

In the $11.3 \mu\text{m}$ band region, instead, the situation is clearly better. In fact for most sources the discrepancies, between theoretical and observational fluxes, are less than 10% and in no case they exceed 25%. In the worse cases the discrepancies appear always in the long wavelength wing of the $11.3 \mu\text{m}$ feature and they are due to the fact that the observed bands are generally wider than the laboratory SiC features. These differences in the width of the bands could possibly be due either to the different temperatures of SiC grains in laboratory and in the circumstellar environments (Goebel et al. 1995) or to the difference between the circumstellar and laboratory grain size distributions.

It is important to note that in our best fitting procedure we have not taken into account some important features present in the spectra of many sources (see Table 1) and that are clearly visible in Fig. 4 (IRAS 05028+0106). This is the case for the depression around $14 \mu\text{m}$ which, together with the strong absorption band at $3 \mu\text{m}$, has been ascribed to C_2H_2 and HCN molecular absorption (Ridgway et al. 1978; Noguchi et al. 1981; Willems 1988a, 1988b). Obviously such bands, as seen in the spectra, are the result of photospheric absorption bands modified by the contribution of the dust emission.

Another feature often seen in the LRS spectra and also visible in Fig 4, is the emission band around $8.6 \mu\text{m}$. Willems (1988a) reports that it is well correlated with the $3 \mu\text{m}$ absorption and is probably of molecular origin. On the other hand Baron et al. (1987) suggest that it may have a solid state origin and a good candidate could be amorphous carbon. Indeed a broad feature around $8.5 \mu\text{m}$ is present in the extinction spectra of the carbon grains produced by Koike et al. (1980) and Bussoletti et al. (1987) but we find that it is generally too weak to explain the band seen in the spectra of carbon stars. In any case all the above features need to be investigated and high dispersion observations could significantly contribute to ascertain the mentioned hypotheses.

The best-fit curve reported in Fig. 4 is again an example of what it may occur in the far infrared region also in other sources of our sample: the observed broad band fluxes at 60 and $100 \mu\text{m}$ are greater than the calculated ones. This could probably be due to the contribution to the emission coming from some interstellar cirrus that in our model is not taken into account.

Starting from the best-fit parameters it is possible to evaluate the total mass of the dust present in the circumstellar envelopes and the mass-loss rates from the central stars, if the stellar radius is known. In this respect we shall assume that the value of R_* is related to the star temperature by means of the empirical relations given by Bergeat et al. (1978). Therefore, as far as the mass of the envelopes is concerned, using the best-fit values of

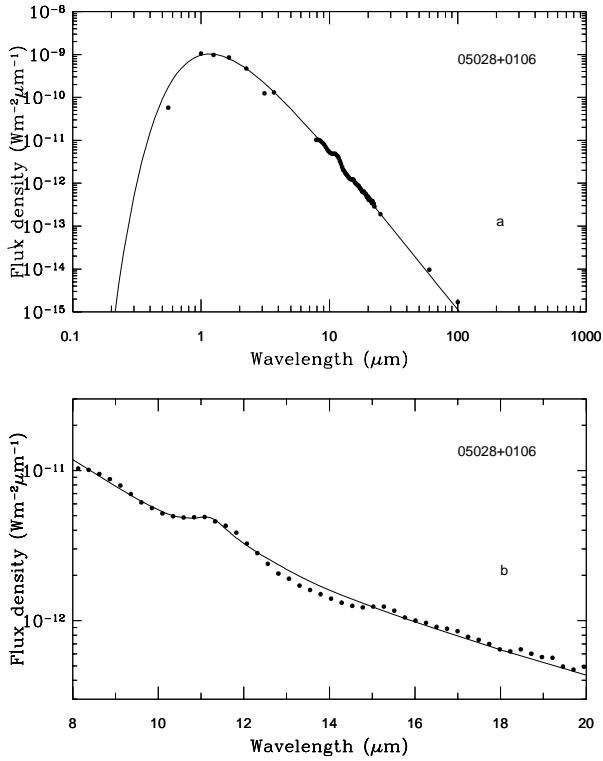


Fig. 4. Best-fit of a source (IRAS 05028+0106) showing the broad absorption bands at 3 and 14 μm and an emission feature around 8.6 μm (see text).

all the parameters listed in Table 2, we can calculate the mass of the dust envelope, due to the i -th component alone:

$$M_i = \frac{16\pi}{3} \frac{\rho_i \tau_i}{\left(\frac{Q_{ext}}{a}\right)_i} \frac{R_E}{R_I} \left(\frac{R_I}{R_*}\right)^2 R_*^2 \quad (1)$$

where ρ_i is the mass density of the grains of that species, τ_i is the optical thickness of the envelope (at the reference wavelength of 5500 \AA) due to the i -th dust component only, while the ratio $(Q_{ext}/a)_i$ is evaluated also at 5500 \AA . The quantity τ_i is obtained from the best-fit values of the total optical thickness τ and the mass percentage of a given component, known its extinction properties. Using Eq. (1) for the three components we have found values of the total dust mass of the envelopes ranging from 2.4×10^{-7} (IRAS 18562+1417) and 1.5×10^{-4} (IRAS 21035+5136) solar masses. For comparison the mass of the envelope around a very evolved carbon star such as IRC+10216 is of the order of 10^{-4} solar masses (Orofino et al. 1990).

On the other hand, starting from the best-fit values of T_* , R_I/R_* and using the empirical relations by Bergeat et al. (1978), we can evaluate the inner radius in absolute units and hence the mass-loss rate for the i -th dust species (Chan & Kwok 1990):

$$\dot{M}_i = C_i \tau_i R_I v \quad (2)$$

where v , assumed equal to 15 km/s (Chan & Kwok 1990), is the stellar wind velocity, while the quantity C_i (constant for

each species) is related to the dust-to-gas ratio Ψ_i through the equation:

$$C_i = \frac{16\pi \rho_d}{3\Psi_i} \left(\frac{Q_{ext}}{a}\right)_i \quad (3)$$

The value of Ψ_i can be obtained using the general expression:

$$\Psi_i = \frac{A_i y_i f_i}{\mu} \quad (4)$$

where A_i is the molecular weight of the grain material, y_i the abundance of the least abundant element in the grain, f_i the fraction of the element condensed in solid form and μ is the mean atomic weight of the gas.

For the AC component we have taken $A = 12$, $y = 5.3 \times 10^{-4}$ (average abundance in carbon stars - Lambert et al. 1986), and $f = 0.5$ (Whittet 1992), while for the SiC component we considered $A = 40$, $y = 3.6 \times 10^{-4}$ (silicon cosmic abundance - Whittet 1992), and $f = 1.0$ (Whittet 1992). Using a mean atomic weight of the gas $\mu = 1.3$ (Chan & Kwok 1990), we obtain from Eq. (4) $\Psi = 2.4 \times 10^{-3}$, for the AC and $\Psi = 1.1 \times 10^{-3}$ for the SiC component. Introducing these values of Ψ together with the mass densities $\rho = 1.87 \text{ g/cm}^3$ for AC and $\rho = 3.2 \text{ g/cm}^3$ for SiC in Eqs. (3) and (2), it is possible to obtain the mass-loss rates for each component and from these, the total ones (see Table 2).

A comparison between our values and the mass-loss rates derived from observations of CO emission lines for the 15 common sources reported by Skinner & Whitmore (1988), shows that the agreement is quite acceptable. In fact, except for a single case (IRAS 03374+6229), the maximum discrepancy between the different values obtained with the two different methods is contained within a factor of 2. Furthermore, when the absolute band strengths of the SiC feature, as defined by Skinner & Whitmore (1988), are plotted against the mass-loss rates found in this work (see Fig. 5), a clear correlation appears (correlation coefficient $r = 0.78$ for the 37 data points relative to the sources for which the distances are independently known). This conclusion confirms the results already found by Skinner & Whitmore (1988) for the same kind of sources.

5. Discussion and conclusions

Let us now discuss our results by considering, from a statistical point of view, the values of the best-fit parameters for all the 55 sources reported in Table 2. In Fig. 6 the temperature of the central star is plotted against the optical thickness. It is evident that a clear anticorrelation (correlation coefficient $r = -0.87$ for 55 data points) exists between the two quantities so that, in general, the thickest envelopes are associated with the coldest stars. In fact the more evolved stars that, due to their long outflow activity, are surrounded by the thickest envelopes, have also the more expanded photospheres and therefore the lowest effective temperatures.

Fig. 7 shows, as a function of the optical thickness, the number distribution of the carbon stars fitted with the two kind of

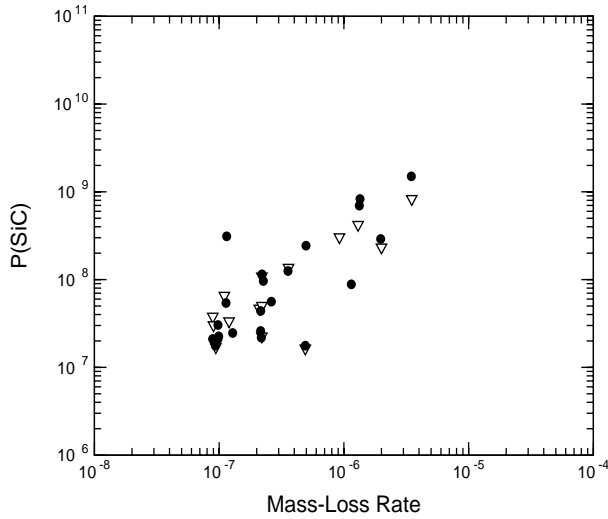


Fig. 5. Band strength of the SiC feature, $P(\text{SiC})$ (in $10^{-26} W_{pc^2 m^{-2} Hz^{-1}}$), plotted against the mass-loss rates (in solar masses per year) as obtained from our model. The band strength data have been taken from Skinner and Whitmore (1988) (triangles) and from Egan & Leung (1991) (dots).

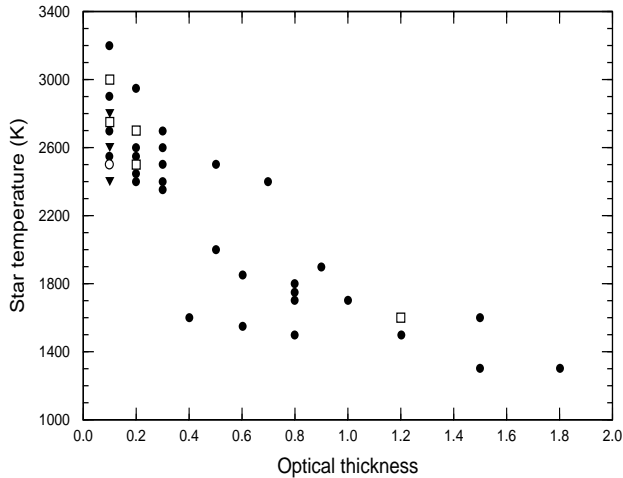


Fig. 6. The central star temperature of the 55 carbon stars plotted against the optical thickness of the circumstellar envelope. A *filled circle* represents a single source, a *square* is for 2 sources, a *triangle* for 3 sources and an *open circle* for 6 sources (see also Table 2)

mixtures composed respectively of AC and α -SiC only (33 objects) and AC with both type of SiC grains (22 objects). From the analysis of this figure and Table 2 we draw the following conclusions:

- a) all the sources, in addition to the AC grains accounting for the continuum emission, need always the presence of α -SiC particles and only some of them require also β -SiC;
- b) in those sources where both types of SiC particles are present and except that for one object (IRAS 20082+2911), the percentage of α -SiC is always greater than that of β -SiC;
- c) the relative mass abundance (SiC/AC) is found to be between ~ 0.1 and 0.3 . These values are in agreement with

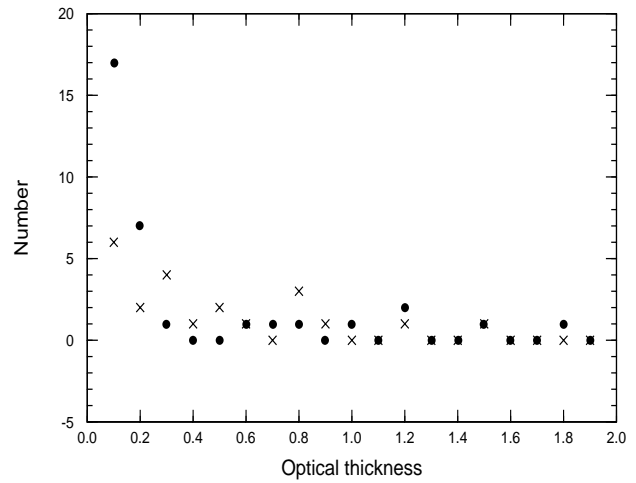


Fig. 7. Number distribution of the carbon stars as a function of the optical thickness of the circumstellar envelope. Dots and crosses represent the number of sources fitted with a mixture composed of AC and α -SiC only and AC with both type of SiC grains respectively

the relative abundances of carbon and silicon in the solid component of the envelopes around carbon stars (Orofino et al. 1991);

- d) the presence of one or both types of SiC particles seems not correlated neither with the total optical thickness (at least for τ greater than 0.1) nor with any other physical and geometrical parameters of the circumstellar envelope. We note, however, that the sources with α -SiC only and $\tau = 0.1$ are 17 out of 33 while those with both types of SiC grains and $\tau = 0.1$ are 6 out of 22.

All the above considerations indicate that around carbon stars α -SiC particles are more abundant and likely to occur than β -SiC grains. This result although somewhat surprising is in general agreement with the findings by other authors (Speck et al. 1996; Groenewegen 1995), but must be reconciled with the lack of α -SiC in meteorites.

As far as the relative abundance (SiC/AC) of the dust components is concerned we note a discrepancy of a factor 5 in the values found in this paper (SiC/AC = 0.3) and by Groenewegen (1995; SiC/AC = 0.06) for the common source IRAS 03229+4721. This can be due mainly to three reasons: 1) the ratio SiC/AC depends on the choice of the dust absorption coefficients (we use two different types of SiC and not one); 2) the free parameters used in the different models are not the same (mainly T_* , R_I and τ) and this influences the grain temperatures and hence the shape and relative intensity of the 11.3 band; 3) most importantly, Groenewegen (1995) uses the implicit assumption that the radii of the two dust grain components are the same. In our case the radius of the SiC particles is much greater than that of the AC grains. This difference influences directly the number density of the two (or three) dust components needed by the models and therefore the relative mass abundance SiC/AC.

As far as the point d) is concerned, if there exists a correlation between the type of SiC and the circumstellar absorption, this is not evidenced from our analysis even if it cannot be excluded for values of the optical thickness lower than $\tau = 0.1$. Concerning this point we recall that Chan & Kwok (1990) suggested that such kind of correlation could be linked with the evolution of carbon stars and to the formation sequence of the SiC component. In fact, they suggest that, due to the different formation temperature of α and β -SiC, there could be a temporal sequence in which the latter is formed once the shell becomes thick enough to lower the temperature in the outer part of the envelope. In the light of our results we think the presence and formation of the β -SiC particles must be linked to other kind of parameters and/or physical processes. To this purpose it is worthwhile to note that in all the sources analysed in this work the temperature of the SiC grains at the inner radius of the circumstellar envelope is always lower than 1500 K, the condensation temperature for SiC reported by Gilman (1969) and McCabe (1983).

In conclusion we have shown that only a thorough analysis, of the type we started in Paper I and extended to a larger sample of carbon stars in this work, can really elucidate the composition and relative amount of the various dust components present in the circumstellar envelopes of a homogeneous set of sources. At the moment we think that the results presented in this paper are the best we can obtain and the limitation is mainly due to both the quality and quantity of observational data. We note for example that, since we could not take into account the variability nature of this class of sources, we cannot exclude a priori a time variation in the composition and/or size distribution of the grains due to the stellar variability.

New observations of improved quality taken at different epochs of the variability cycle can be of great help since, at present, the resolution and the signal to noise (S/N) ratio of the observed spectra are worse than those achieved for the laboratory data. In this respect we hope that the ISO data which will come soon will be of great help in this direction. On the other hand experimental work is needed to account for other possible components of the dust mixture and to better reproduce the real grain size distribution.

Acknowledgements. We thank an unknown referee whose comments and suggestions helped us to improve the quality of the paper. This work was supported by CNR-GIFCO, ASI and MURST

References

- Amari S., Hoppe P., Zinner E., Lewis R. S., 1992, ApJ 394, L43
 Baron Y., de Muizon M., Papoular R., Pégourié B., 1987, A&A 186, 271
 Beckwith S., 1985, in: Mass Loss from Red Giants, M. Morris, B. Zuckerman (eds.) Reidel, Dordrecht, p. 95
 Beichman C.A., Neugebauer G., Habin H.J., Clegg P.E., Chester T.J., 1988, IRAS Catalogs and Atlases - Explanatory Supplement, NASA R.P. 1190
 Bergeat J., Sibille F., Lunel M., 1978, A&A 64, 423
 Blanco A., Borghesi A., Fonti S., Orofino V., 1994, A&A 283, 561 (Paper I)
 Borghesi A., Bussoletti E., Colangeli L., De Blasi C., 1985, A&A 153, 1
 Borghesi A., Bussoletti E., Colangeli L., et al., 1986, Infrared Phys. 26, 37
 Bussoletti E., Colangeli L., Borghesi A., Orofino V., 1987, A&AS 70, 257
 Chan S. J., Kwok S., 1988, ApJ 334, 362
 Chan S. J., Kwok S., 1990, A&A 237, 354
 Dischler B., Bubenzer A., Koidl P., 1983a, Appl. Phys. Lett. 42, 636
 Dischler B., Bubenzer A., Koidl P., 1983b, Solid State Comm. 48, 103
 Egan M.P., Leung C.M., 1991, ApJ 383, 314
 Egan M.P., Leung C.M., Spagna G.F. Jr., 1988, Comput. Phys. Commun. 48, 271
 Gezary D.Y., Schmitz M., Mead J.M., 1987, Catalog of Infrared Observations, Part II - Appendix E, NASA R.P. 1196
 Gilman R.C., 1969, ApJ Letters 155, L185
 Goebel J.H., Cheeseman P., Gerbault F., 1995, ApJ 449, 246
 Groenewegen M.A.T., 1995, A&A 293, 463
 Groenewegen M.A.T., de Jong T., 1991, ESO Messenger 66, 40
 Hoffleit D., Jaschek C., 1982, The Bright Star Catalog, 4th rev. ed., Yale University Observatory, New Haven
 Hoppe P., Amari S., Zinner E., Ireland T., Lewis R.S., 1994, ApJ 430, 870
 IRAS Science Team, 1986, IRAS Catalogs and Atlases: Atlas of Low Resolution Spectra, A&AS 65, 607
 Jura M., 1985, in: Interrelationship Among Circumstellar, Interstellar and Interplanetary Dust, Nuth J. A., Stencel R. E. (eds.) NASA CP 2403, p. 3
 Keenan P.C., Morgan W.W., 1941, ApJ 94, 501
 Knapp G. R., Morris M., 1985, ApJ 292, 640
 Koike C., Hasegawa H., Manabe A., 1980, Ap&SS 67, 495
 Kömpe C., Gürtler J., Henning Th., 1995, Ap&SS 224, 353
 Lambert D.L., Gustafsson B., Eriksson K., Hinkle K.H., 1986, ApJSS 62, 373
 Le Bertre T., 1988, A&A 203, 85
 Leung C.M., 1975, ApJ 199, 340
 Leung C.M., 1976a, J. Quant. Spectro. Rad. Trans. 16, 559
 Leung C.M., 1976b, ApJ 209, 75
 McCabe E. M., 1983, MNRAS 200, 71
 Neugebauer G., Leighton R.B., 1969, The Two-Micron Sky Survey, NASA SP-3047, Washington, DC
 Noguchi K., Kawara K., Kobayashi Y., et al., 1981, PASJ 33, 373
 Orofino V., Colangeli L., Bussoletti E., Blanco A., Fonti S., 1990, A&A 231, 105
 Orofino V., Mennella V., Blanco A., et al., 1991, A&A 252, 315
 Pégourié B., 1988, A&A 194, 335
 Price S.D., Murdock T.L., 1983, The Revised Air Force Geophysical Laboratory Sky Survey Catalog, AFGL-TR-83-0161
 Ridgway S.T., Carbon D.F., Hall D.N.B., 1978, ApJ 225, 138
 Rouleau F., Martin P.G., 1991, ApJ 377, 526
 Skinner C.J., Whitmore B., 1988, MNRAS 234, 79P
 Speck A.K., Barlow M.J., Skinner C., 1996, in: From Stardust to Planetesimals, Kress M.E., Tielens A.G.G.M., Pendleton Y.J. (eds) NASA CP 3343, p. 61
 Stephenson, C.B., 1989, A General Catalogue of Cool Galactic Carbon Stars, Publ. Warner and Swasey Obs. I, 2nd Edition, Vol. 3, No. 2
 Tang M., Anders E., 1988, Geochim. Cosmochim. Acta 52, 1235
 Tielens A.G.G.M., 1990, in: Carbon in the Galaxy: Studies from Earth and Space, Tarter J., Chang S., DeFrees D.J. (eds.) NASA C. P. n. 3061, p. 59

- Tielens A.G.G.M., Allamandola L.J., 1987, in: Physical Processes in Interstellar Clouds, G.E. Morfill, M. Scholer (eds.) Reidel, Dordrecht, p. 333
- Whittet D.C.B., 1992, Dust in the Galactic Environment, Institute of Physics Publishing, Bristol, United Kingdom
- Willems F. J., 1988a, A&A 203, 51
- Willems F. J., 1988b, A&A 203, 65
- Yamashita Y., 1972, Ann. Tokyo Astr. Obs. 13, 169
- Yamashita Y., 1975, Ann. Tokyo Astr. Obs. 15, 1
- Zinner E., Tang M., Anders E., 1989, Geochim. Cosmochim. Acta 53, 3573